Electronic Supplementary Material (ESI) for Journal of Materials Chemistry A.

Morphogenesis of Cement Hydrate

S. E. Moghaddam,[1,2,3] V. Hejazi,[1,4] S. Hwang,[1] S. Srinavasan,[1] J. Miller,[4] B. Shi,[1] S. Zhao,[1] I. Rusakova,[5] A. Alizadeh,[4] K.H. Whitmire,[2,3] R. Shahsavari[1,3,6]*

[1]Department of Civil and Environmental Engineering, Rice University, Houston, TX 77005

[2]Department of Chemistry, Rice University, Houston, TX 77005

[3] The Smalley-Curl Institute, Rice University, Rice University, Houston, TX 77005

[4]C-Crete Technologies LALC, 8973 Interchange Drive, Houston, TX 77054

[5]Texas Center for Superconductivity and Advanced Materials, University of Houston Science Center, Houston, TX 77004

[6]Department of Material Science and Nano Engineering, Rice University, Houston, TX 77005

Supplementary Information

Supplementary Information 1. Time-dependent spectroscopic study of the reaction Kinetic

In Figure S1 the absorption spectra of Calcium nitrate and sodium silicate before and after mixing in water are compared. The absorption was measured during the first 65 min of reaction more than ten times. The graph shows that after adding calcium solution to silicate, the intensity increases after the first few minutes and three new peaks at 210, 270 and 320 appear. After around 25 minutes the changes decrease, demonstrating the main part of reaction takes place at the first 25 min of mixing raw materials. Since the sonication power can increase the rate of reaction and in view of the aforementioned UV-Vis results, we used the 60-100 min reaction time for all of our experiments, except in the case of dilute solutions (using 200 mL water) where the reactions were performed for 6 h.

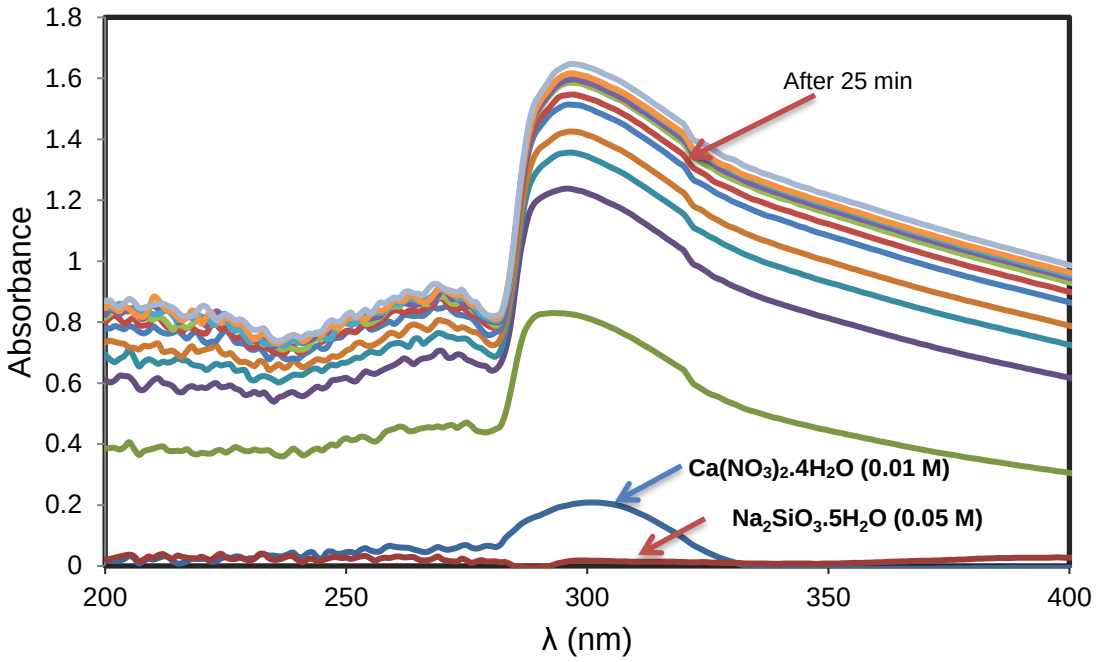

Figure S1. Kinetic of reactions. UV-Vis absortion of sodium metasilicate pentahydrate (0.05 M) and calcium nitrate tetra hydrate (0.1 M) befor and after adding calcium to silicate solution. UV-Vis of solution was taken during 65 min for 12 times.

Supplementary Information 2. Sonication versus Stirring

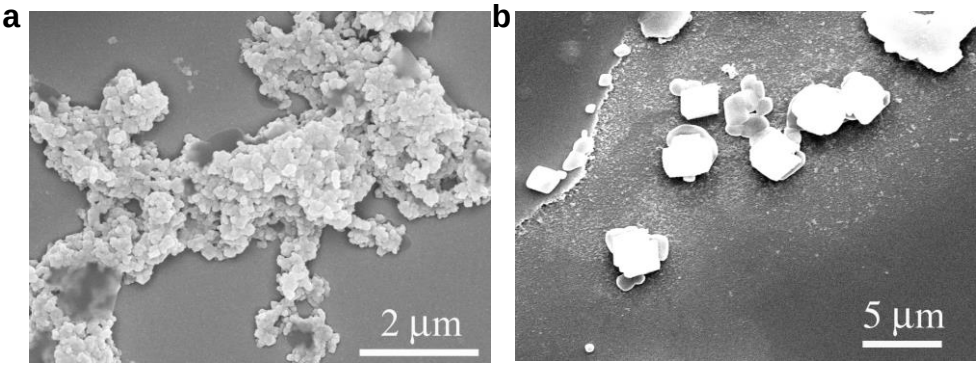

Figure S2. Comparison of the reaction of sodium metasilicate pentahydrate and calcium nitrate tetrahydrate. Reaction conducted via stirring **(a)** and sonication **(b)** methods.

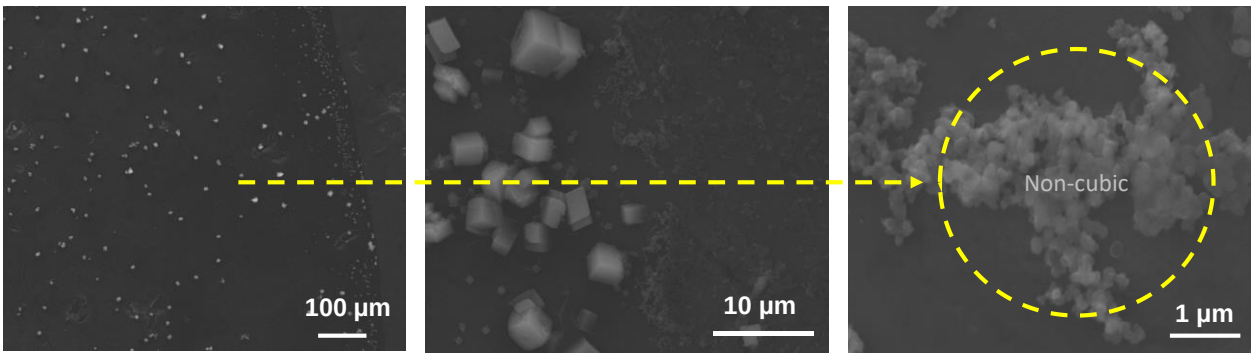

Figure S3. Cubic to non-cubic ratio. SEM images of product: Left to right from low magnification to high magnification.

Supplementary Information 3. Impact of electron beam on the C-S-H particles

The exposure to the high energy electron beam damages the samples making the high-resolution imaging challenging. After a short exposure to the beam, the exposed area melts and converts into an amorphous phase (Figure S4). Similar instability under the electron beam has been reported previously.[1] C-S-H crystals have a very limited lifetime under the beam as a result of dehydration, and melt to yield an amorphous product.

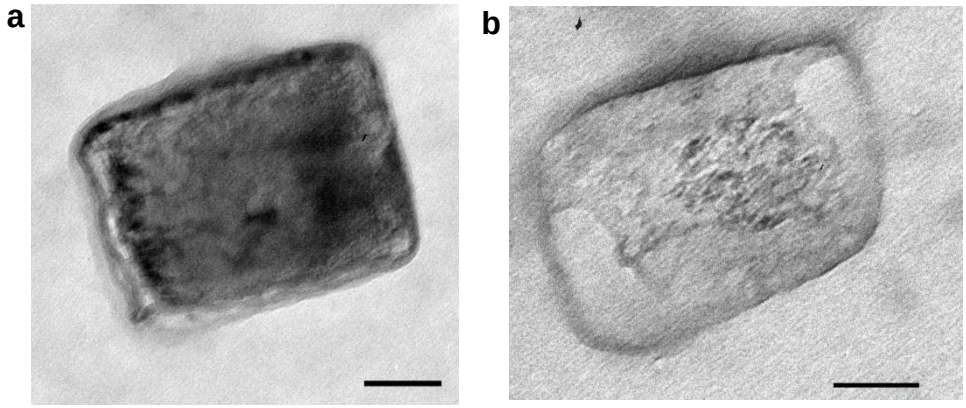

Figure S4. TEM images of a molten C-S-H particle. After few seconds **(a)** and after 2 minutes **(b).** Scale bars are 500 nm.

Supplementary Information 4. FT-IR study of C-S-H samples

The C-S-H particles were characterized by IR spectroscopy which is a useful tool to study the local structure of solids. In this study the mid-IR spectrum (frequency range 4000-400 Cm^{-1}) was collected for powdered sample. Figure S5 illustrates the FT-IR spectra of the synthesized C-S-H with starting Ca/Si ratio of 1.5. The presence of intense, sharp peak at ~970 cm^{-1} is due to the Si–O stretching vibrations. This, combined with the Si–O–Si bending bands at ~667 cm^{-1} indicates the formation of C-S-H structures.[2] The broad groups of peaks in the range of 1420 -1480 cm^{-1} are the characteristic bands for the asymmetric stretching of ($v3$) CO_3^{2-} group, and the weak shoulder at ~870 cm^{-1} is due to the out-of-plane bending ($v2$) of CO_3^{2-}.[3] The band at 1640 cm^{-1} corresponds to H-O-H bending vibration of molecular H_2O. The broad bands at 2900-3600 cm^{-1} are attributed to the stretching vibration of O-H groups in H_2O or hydroxyls with a wide range of hydrogen bond strengths. Weak bands are observed at 2867, and 2924 cm^{-1} for the contamination of CTAB in C-S-H product.[4] The silicate vibration regions of this C-S-H sample generally resemble the reported[5] spectrum of 1.4 nm tobermorite which has mostly Q^2 sites in the range of 900-1060 cm^{-1}, consistent with our ^{29}Si MAS NMR data, suggesting that the product contains mostly Q^2.

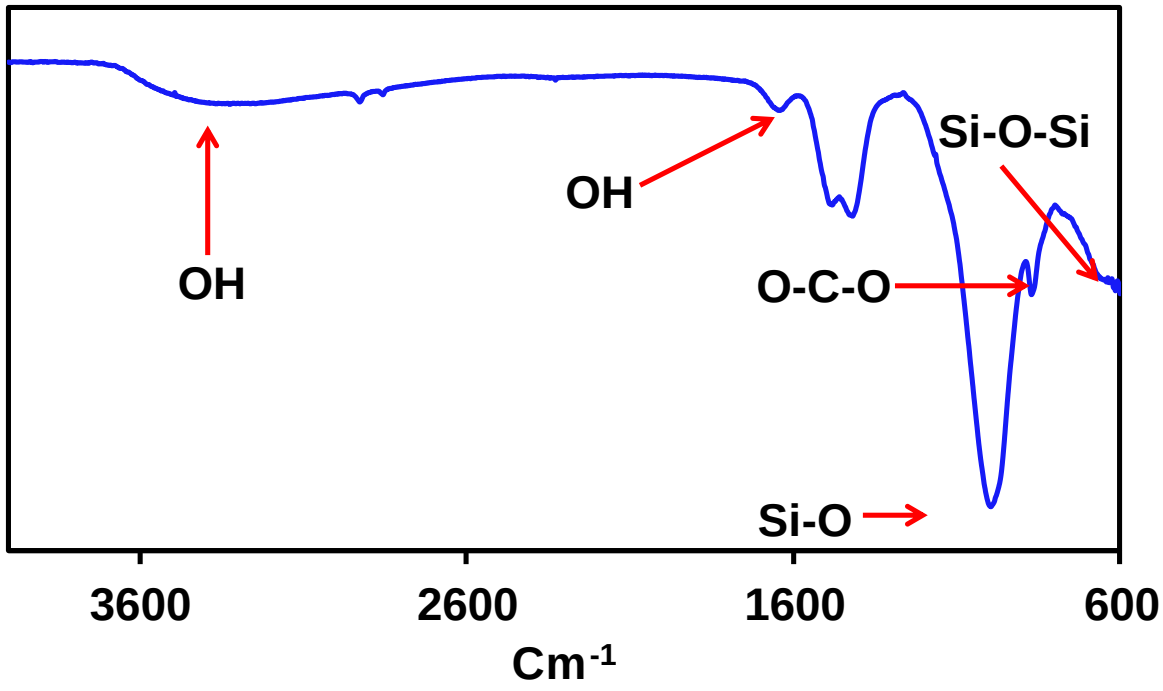

Figure S5. FT-IR study. Spectrum of C-S-H particles synthesized from CTAB, and Ca/Si of 1.5.

Supplementary Information 5. C-S-H synthesis under CO_2 gas flow

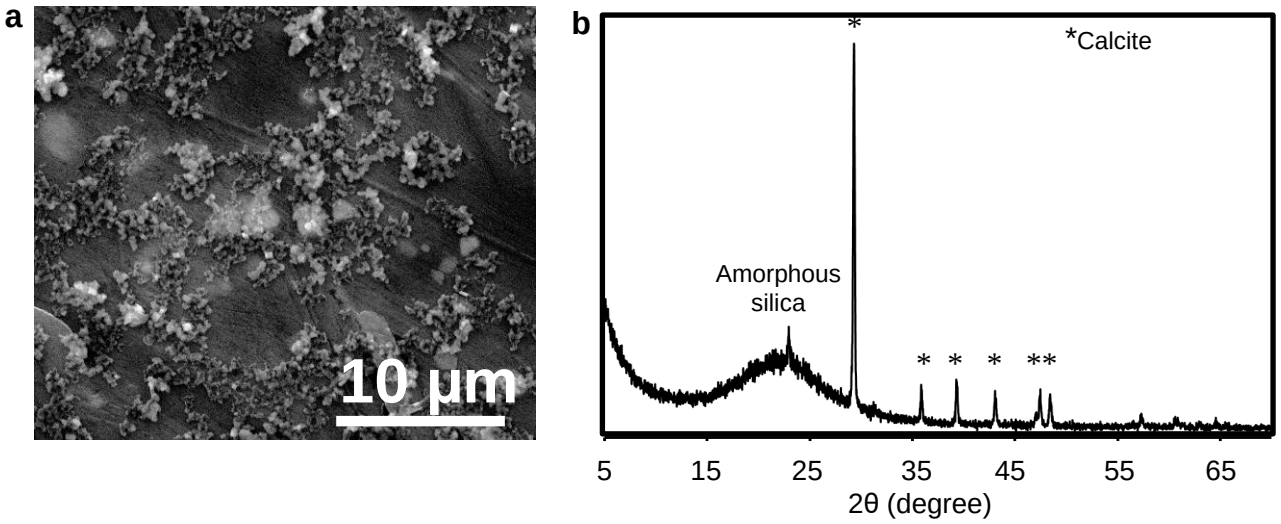

Figure S6. Precipitation under carbon dioxide bubbling. a, SEM image of particles. **b,** The XRD pattern of precipitate under carbon dioxide bubbling, indicating formation of amorphous silica and calcite.

Supplementary Information 6. C-S-H synthesis under N_2 gas flow

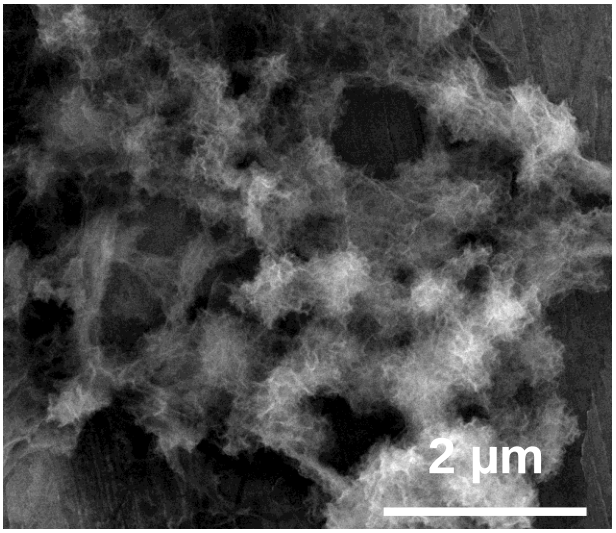

Figure S7. SEM image of C-S-H particles synthesized under N_2.

Supplementary Information 7. Elemental analysis on cut particles

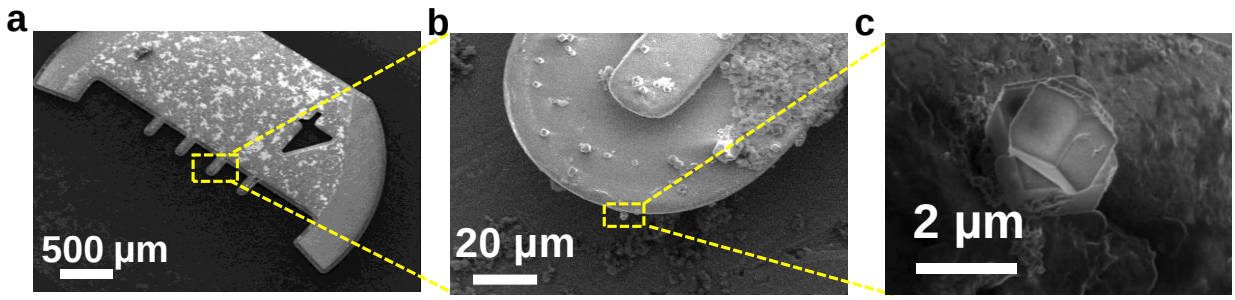

Figure S8. FIB sample preparation for TEM-EDS a, Cubic particles deposited on a FIB-TEM half grid. **b,** A single cubic particle deposited on the tip of post No. 3 of the half grid. **c,** Front view of the cubic particle on the post (SEM showed a small cubic particle sat on the top of a larger cubic particle).

Supplementary Information 8. C-S-H synthesis in the presence of calcite seed as an additive under inert gas

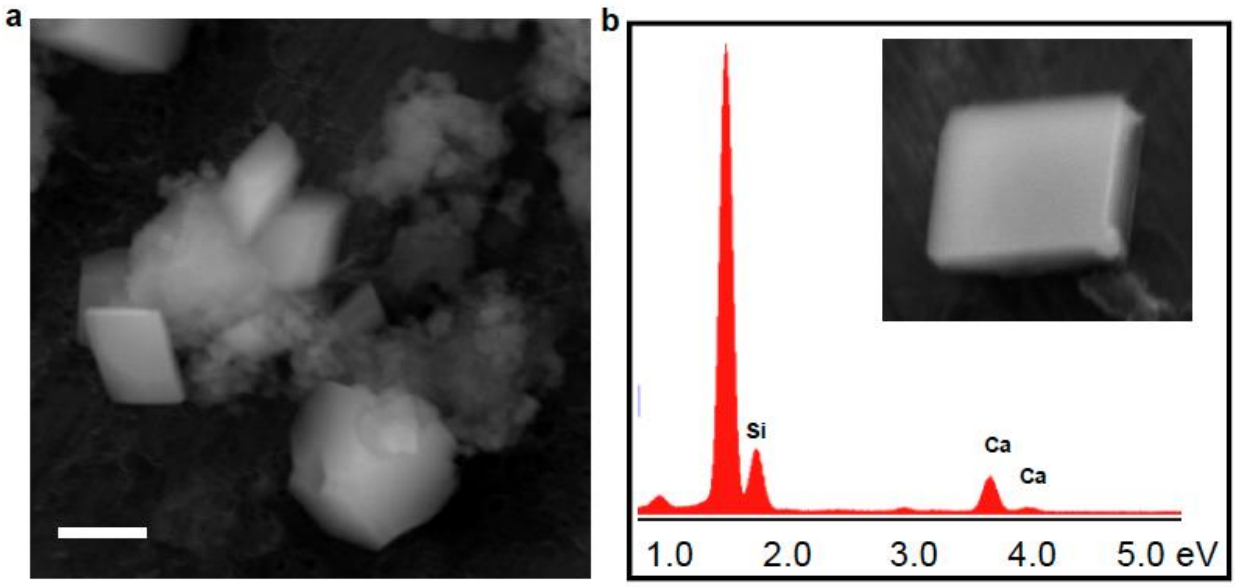

Figure S9. a, The product of reaction in the presence of calcite seeds under Ar. **b,** EDS spectra of cubic particle in inset which is ~10 times larger than starting calcite seeds. Scale bar is 1 µm.

Supplementary Information 9. Morphogenesis of C-S-H

Samples with relatively high silicate precursor concentrations of 10 and 20 mM resulted in almost double the amount of C-S-H in the first 30 to 60 min of the reaction (monitored by UV-Vis), compared to the reaction with lower precursor concentration of 2.5 mM. Moreover, while the reaction from concentrated starting precursors seemed complete after 90 min, the reaction involving 2.5 mM precursor concentration had only finite amount of product in the same period of time. Increasing the time of sonication can be effective in growth of crystalline phases and enhance the yield of the reaction.[6] Thus, the latter reaction was placed in the sonication bath for an additional 4h to obtain the final product. Then, an abrupt transition in morphology was observed with decreasing precursor concentration from 20 to 2.5 mM, irrespective of the choice of Ca to Si ratio. In contrast to the cubic C-S-H NPs obtained with 20-5 mM of precursor concentration (Fig. 1a-c and Fig. 3a-f in the main manuscript), large core/shell-like at Ca/Si of 1.0 (Fig. 3g in the main manuscript) and dendritic assembled shaped particles at Ca/Si of 1.5 and 2.0 (Fig. 3h and i in the main manuscript) were formed. The XRD pattern confirmed the assignment of the product to a C-S-H phase in all samples (Figure S10). However, XRD patterns of samples synthesized in dilute solution showed a higher concentration of calcite due to longer reaction time and higher volume of solvent which stimulate the higher dissolution of the carbonate anion. Additional peaks related to portlandite (CH) are also observed in the XRD pattern of C-S-H at 2.5 mM of precursor concentration and Ca/Si ratio of 1.5 and 2.0.

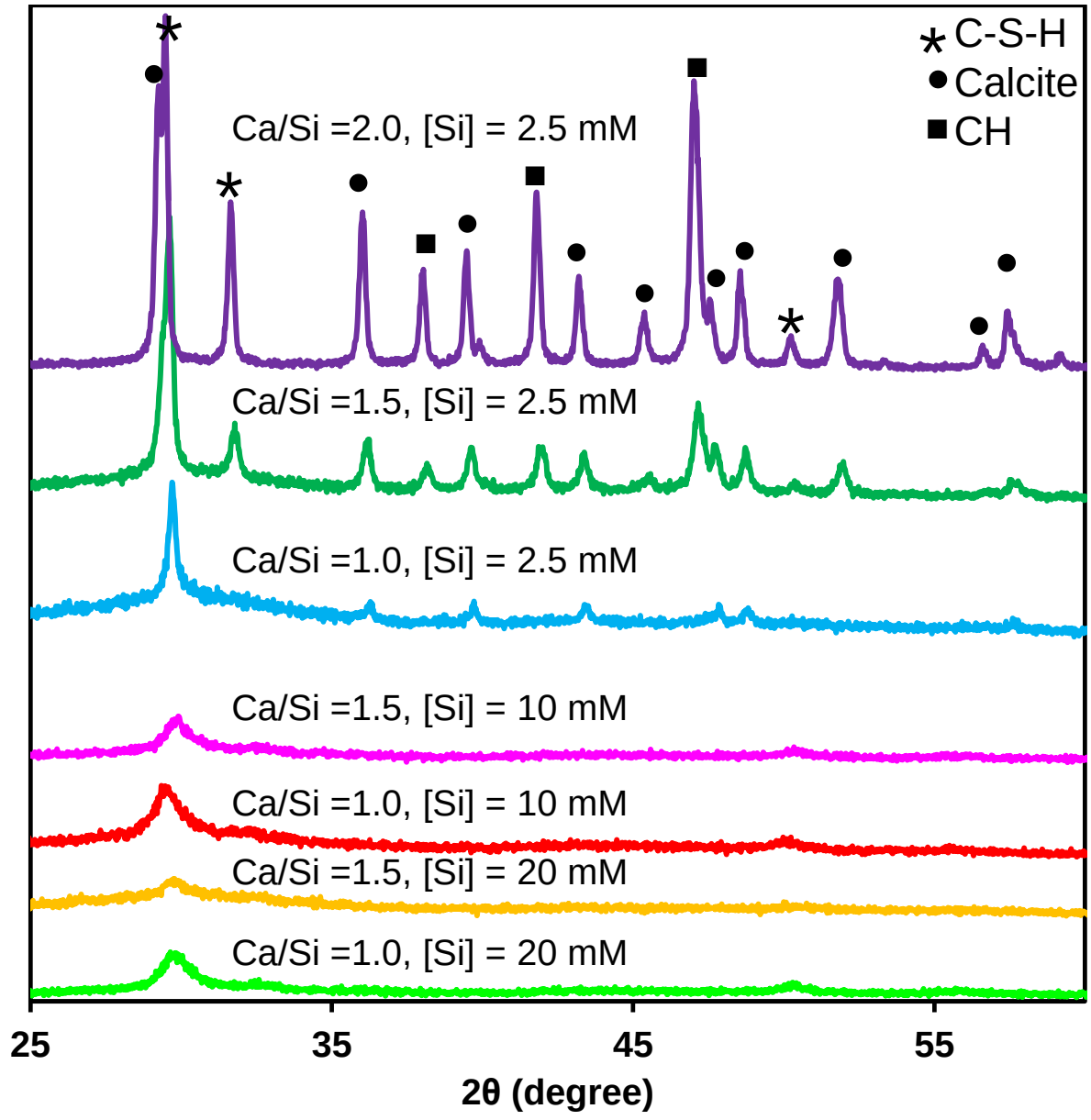

Figure S10. XRD pattern of samples synthesized under different precursors concentrations.

Supplementary Information 10. Cationic versus Anionic Surfactants

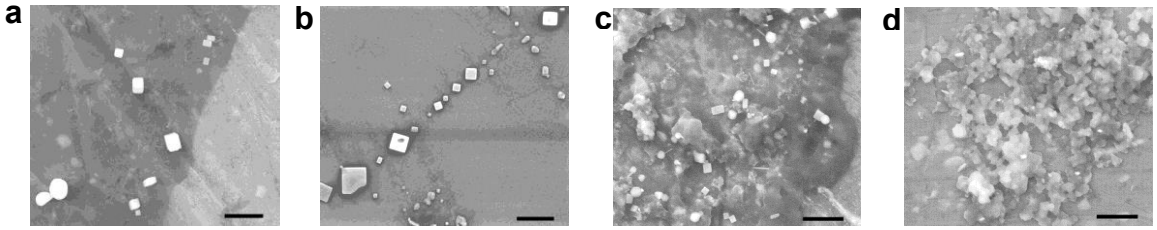

Figure S11. SEM images of C-S-H synthesized in the presence of cationic and anionic surfactants. a, CTAB. **b,** CPB. **c,** TDAB. **d,** SDS. Scale bars show 5 μm.

Supplementary Information 11. Particle Formation by Varying Counter-Ions in the Calcium Precursor.

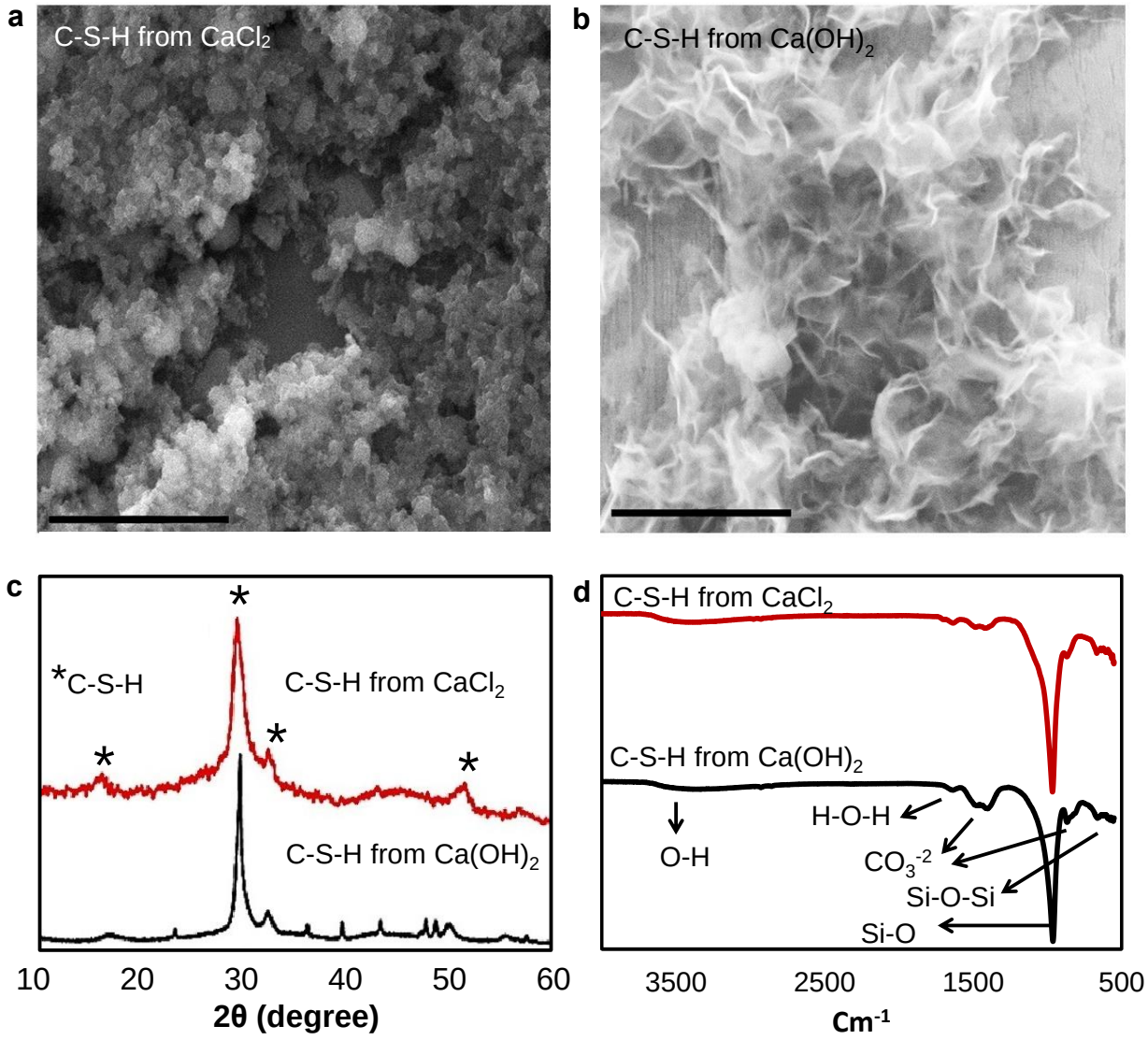

Figure S12. C-S-H synthesized in the presence of different calcium salts (Ca/Si=2.0). a-b, SEM images of the C-S-H synthesized from $Na_2SiO_3 \cdot 5H_2O$ and $Ca(Cl)_2$ **(a),** and $Ca(OH)_2$ **(b**) in the presence of CTAB, in 100 mL CO_2 free dI-water ([CTAB]=0.8 mM). All scale bars show 1 μm. **c,** Powder-XRD pattern of the C-S-H (*): $CaCl_2$ (Red), $Ca(OH)_2$ (Black). **d,** FT-IR spectra of C-S-H samples: $CaCl_2$ (Red), $Ca(OH)_2$ (Black).

Supplementary Information 12. Nanoindentation and Porosity Analysis Results.

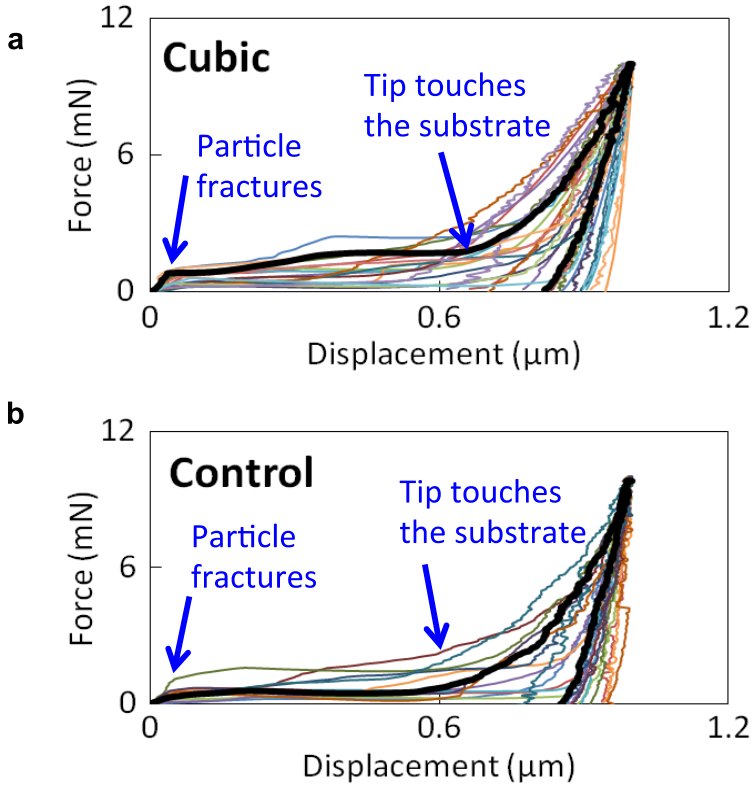

Figure S13. Load-displacement curves of individual cubic and control C-S-H particles. **a,** cubic and **b**, control particles indented using flat-end tip. The various colors represent indentation of several independent particles and the black color is a typical representative load-displacement plot.

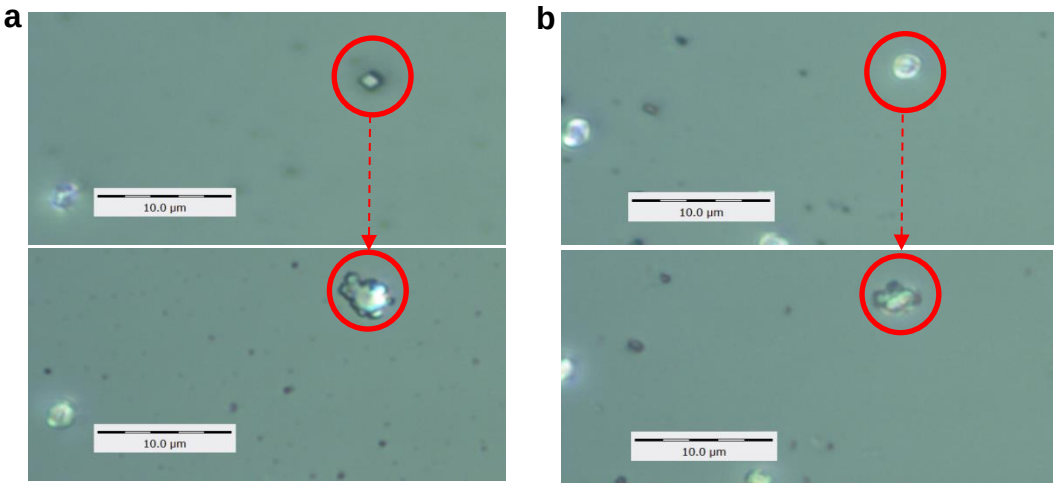

Figure S14. Optical image of cubic **(a)** and control **(b)** particles indented with a flat end tip: before (Top images) and after (bottom images) indentation. The magnification of the optical microscope is 100X.

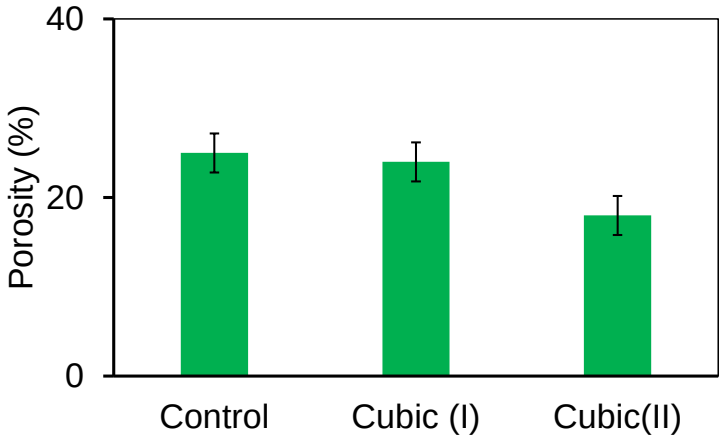

Figure S15. Porosity of compacted cubic and control samples.

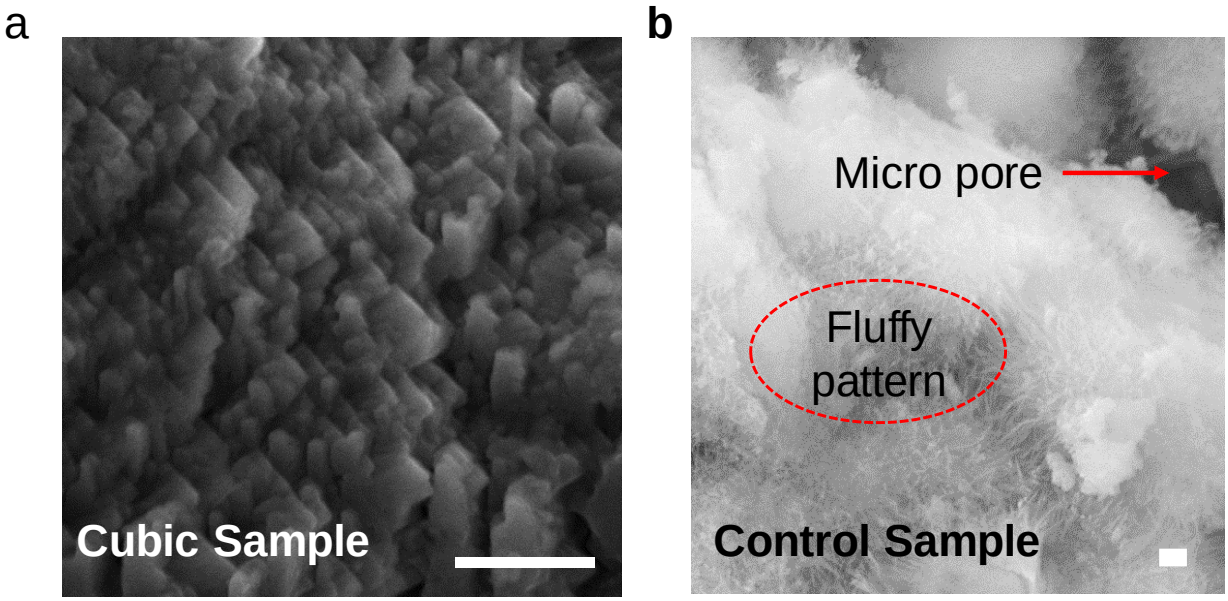

Figure S16. SEM of compacted sample. a, cubic C-S-H and **b**, Control (hydrated alite). particles from side view on a broken piece. Scale bars show 0.5 μm.

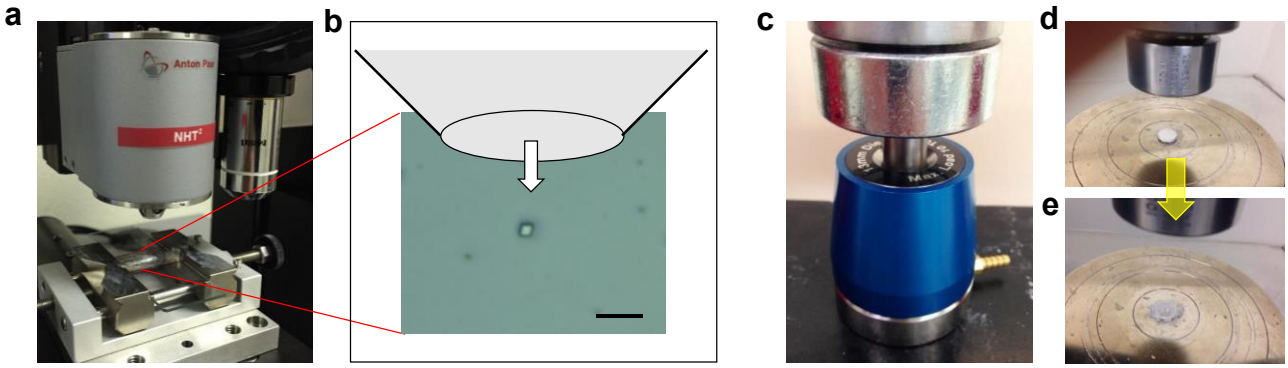

Figure S17. Nanoindentation and compression test set up. a, Anton-Paar Indenter and 100X optical microscope. **b,** Zoom in image of sample on glass slide before indentation. **c,** Pellet press assembly. **d,** Pellet in Instron compression test set-up before compression. **f**, after compression.

Reference

1 Grangeon, S. *et al.* On the nature of structural disorder in calcium silicate hydrates with a calcium/silicon ratio similar to tobermorite. *Cement and Concrete Research* **52**, 31-37 (2013).

2 Mojumdar, S. C. & Raki, L. Synthesis, thermal and structural characterization of nanocomposites for potential applications in construction. *Journal of Thermal Analysis and Calorimetry* **86**, 651-657, doi:10.1007/s10973-006-7720-1 (2006).

3 Mehrali, M. *et al.* Facile synthesis of calcium silicate hydrate using sodium dodecyl sulfate as a surfactant assisted by ultrasonic irradiation. *Ultrasonics Sonochemistry* **21**, 735-742 (2014).

4 Beaudoin, J. J., Dramé, H., Raki, L. & Alizadeh, R. Formation and characterization of calcium silicate hydrate–hexadecyltrimethylammonium nanostructure. *Journal of Materials Research* **23**, 2804-2815 (2008).

5 Yu, P., Kirkpatrick, R. J., Poe, B., McMillan, P. F. & Cong, X. Structure of Calcium Silicate Hydrate (C-S-H): Near-, Mid-, and Far-Infrared Spectroscopy. *Journal of the American Ceramic Society* **82**, 742-748 (1999).

6 Wu, Z., Borretto, E., Medlock, J., Bonrath, W. & Cravotto, G. Effects of Ultrasound and Microwaves on Selective Reduction: Catalyst Preparation and Reactions. *ChemCatChem*, n/a-n/a, doi:10.1002/cctc.201402221 (2014).